J. Phys.: Condens. Matter **23** (2011) 254212 (6pp) doi:10.1088/0953-8984/23/25/254212

Inelastic neutron and low-frequency Raman scattering in niobium-phosphate glasses: the role of spatially fluctuating elastic and elasto-optic constants

A Schulte[1], W Schirmacher[2,3], B Schmid[2] and T Unruh[4,5]

[1] Department of Physics and College of Optics and Photonics, University of Central Florida, Central Florida Boulevard, Orlando, FL 32816-2385, USA
[2] Institut für Physik, Universität Mainz, Staudinger Weg 7, 55099 Mainz, Germany
[3] Physik-Department E13, Technische Universität München, James-Franck-Strasse 1, D-85747 Garching, Germany
[4] Neutronenquelle 'Heinz Maier-Leibnitz' (FRM II), Technische Universität München, D-85747, Garching, Germany
[5] Lehrstuhl für Kristallographie und Strukturphysik, Friedrich-Alexander-Universität Erlangen-Nürnberg, Staudtstraße 3, D-91058 Erlangen, Germany

E-mail: afs@physics.ucf.edu

Received 19 January 2011, in final form 5 March 2011
Published 8 June 2011
Online at stacks.iop.org/JPhysCM/23/254212

Abstract
We investigate the low-frequency enhancement of vibrational excitations ('boson peak') in niobium-phosphate glasses through the combination of inelastic neutron and polarization-resolved Raman scattering. The spectra of these glasses reveal an enhancement of the vibrational density of states and of the cross section for spontaneous Raman scattering in the frequency range below 150 cm^{-1}. A recent theoretical model that is based on fluctuating elastic and elasto-optic (Pockels) constants provides a unified description of the measured neutron and Raman spectra, including the depolarization ratio.

(Some figures in this article are in colour only in the electronic version)

1. Introduction

Inelastic neutron and low-frequency light scattering are efficient probes of low-frequency excitations in glasses [1–3]. While neutron scattering is coupled to density fluctuations the coupling of light involves fluctuations of the dielectric susceptibility. The structural disorder in glasses manifests itself in fluctuations of the elastic properties and the coupling to the respective probe. A spectral enhancement ('boson peak') in the 1 THz (or 100 cm^{-1}) regime is universally observed in the density of vibrational states (DOS) as revealed by neutron scattering. On the other hand, the light-vibration coupling plays another important role, as it controls the absolute value of the effect as seen by light scattering.

Glasses with broad and intense Raman-active modes have attracted attention for applications in all-optical amplification systems as the Raman-gain coefficient depends significantly on the cross section for spontaneous Raman scattering [4]. Therefore it is advantageous to have a material with a smooth and not too small Raman spectrum down to the low-frequency regime.

Concerning the boson peak, an extended literature exists, in which the nature of the vibrational state in this frequency regime has been investigated by experiment and simulation, as well as by theoretical modelling [5–14]. However the light-vibrational coupling was hitherto discussed in terms of a phenomenological frequency-dependent function $C(\nu)$, and it was assumed that this function entered the prefactor of the Shuker–Gammon formula [1, 15]

$$I(\nu) = [n(\nu) + 1]C(\nu)\frac{g(\nu)}{\nu}, \qquad (1)$$

where $n(\nu) = 1/[e^{h\nu/k_B T} - 1]$ is the boson occupation number and $g(\nu)$ is the vibrational density of states. As this function was unknown, many studies have tried to determine it by comparing Raman data with DOS data extracted from specific heat or neutron scattering measurements [16, 17]. Only very recently have two of the present authors developed a theoretical model, in which the light-vibration coupling is modelled by spatially fluctuating Pockels constants, thereby allowing for the violation of the local momentum and angular-momentum selection rules [18]. The vibrational spectrum of the disordered solid was modelled by generalizing elasticity theory to allow for spatial fluctuations of the shear modulus [12–14]. A theory for light scattering needs model assumptions for the coupling of the local polarizabilities to the local strains (elasto-optical coupling, Pockels coupling). Including spatially fluctuating Pockels constants allowed closed expressions to be obtained for the Raman spectrum and thereby the treatment of neutron, Raman, and inelastic x-ray scattering on the same footing. The theory accounts for the differences in the 'boson peak' as seen by Raman scattering compared to neutron scattering.

In this contribution we present a combined experimental and theoretical investigation of low-frequency vibrational excitations in $20Nb_2O_5$–$80NaPO_3$ and $40Nb_2O_5$–$60NaPO_3$ glasses. These materials show a broad and intense Raman spectrum, and they are therefore good candidates for all-optical Raman-gain applications [19]. We employ inelastic neutron scattering as well as polarization-resolved low-frequency Raman scattering in order to explore the role of fluctuations in both the elastic medium and the coupling to light. By applying the theory of [18] we show that the neutron and Raman spectra can be reconciled. The analysis yields information on the light-vibration coupling and the state of disorder of the material. In particular, the depolarization ratio is directly related to fluctuations in the elasto-optic (Pockels) constants.

2. Theoretical background

We briefly review our theoretical framework. We model the disordered solid as an elastic continuum, allowing for spatial fluctuations of the shear modulus G. The statistical properties of the fluctuations $\Delta G(\mathbf{r}) = G(\mathbf{r}) - \langle G\rangle$ are represented by the correlation function

$$C_G(\mathbf{r}) = \langle \Delta G(\mathbf{r}+\mathbf{r}_0)\Delta G(\mathbf{r}_0)\rangle \equiv \langle \Delta G^2\rangle e^{-\frac{1}{4}r^2/\xi_G^2}. \quad (2)$$

This can be shown [12–14, 18] to lead to frequency-dependent complex sound velocities

$$v^2_{\mathrm{L,T}}(\omega) = v^2_{\mathrm{L,T},0} - \Sigma_{\mathrm{L,T}}(\omega), \quad (3)$$

where $\omega = 2\pi\nu$, and $\Sigma_{\mathrm{T}}(\omega) = \frac{1}{2}\Sigma_{\mathrm{L}}(\omega) \equiv \Sigma(\omega)$ is the so-called self-energy. The latter obeys the self-consistent equation (self-consistent Born approximation, SCBA)

$$\Sigma(\omega) = \gamma \int_{|\mathbf{k}|<k_{\mathrm{D}}} \frac{\mathrm{d}^3\mathbf{k}}{(2\pi)^3}\tilde{C}_G(k)[\chi_{\mathrm{L}}(\mathbf{k},\omega) + \chi_{\mathrm{T}}(\mathbf{k},\omega)] \quad (4)$$

where we have put $C_G(k) = f_G\tilde{C}_G(k)$ with $\frac{1}{8\pi^3}\int_{|\mathbf{k}|<k_{\mathrm{D}}} \mathrm{d}^3\mathbf{k}\tilde{C}_G(k) = 1$ and $\gamma \propto f_G \propto \langle\Delta G^2\rangle$. The longitudinal and transverse strain susceptibilities $\chi_{\mathrm{L,T}}$ are

$$\chi_{\mathrm{L,T}}(\mathbf{k},\omega) = k^2 G_{\mathrm{L,T}}(\mathbf{k},\omega) = \frac{k^2}{-\omega^2 + k^2[v^2_{\mathrm{L,T}}(\omega)]}. \quad (5)$$

The DOS is given by

$$g(\omega) = \frac{2\omega}{3\pi}\int_{|\mathbf{k}|<k_{\mathrm{D}}} \frac{\mathrm{d}^3\mathbf{k}}{(2\pi)^3}\,\mathrm{Im}\{G_{\mathrm{L}}(\mathbf{k},\omega) + 2G_{\mathrm{T}}(\mathbf{k},\omega)\}. \quad (6)$$

For the description of the light-vibration coupling the dielectric tensor is expanded with respect to the strain tensor $u_{ij} = (1/2)[\partial_i u_j + \partial_j u_i]$ as $\Delta\epsilon_{ij}(\mathbf{r},t) = a_1(\mathbf{r})\sum_\ell u_{\ell\ell}(\mathbf{r},t)\delta_{ij} + a_2(\mathbf{r})v_{ij}(\mathbf{r},t)$, with $v_{ij} = u_{ij} - (1/3)\delta_{ij}\sum_\ell u_{\ell\ell}$ [20]. These quantities are now assumed [21] to have disorder-induced fluctuations $a_{1,2}(\mathbf{r}) = a^{(0)}_{1,2} + \Delta a_{1,2}(\mathbf{r})$ with correlation functions $C_{1,2}(\mathbf{r}) = \langle\Delta a_{1,2}(\mathbf{r}_0+\mathbf{r})\Delta a_{1,2}(\mathbf{r}_0)\rangle$. The constant terms $a^{(0)}_{1,2}$ produce the usual formulae for Brillouin scattering and Raman scattering. From the fluctuating terms one obtains

$$I_{\mathrm{VH}}(\omega) = [n(\omega)+1]\frac{\alpha}{15}\left(\chi_{2,\mathrm{L}}(\omega) + \frac{3}{2}\chi_{2,\mathrm{T}}(\omega)\right)$$
$$I_{\mathrm{VV}}(\omega) = \tfrac{4}{3}I_{\mathrm{VH}}(\omega) + \alpha[n(\omega)+1]\chi_{1,\mathrm{L}}(\omega) \quad (7)$$

with the partial Raman susceptibilities ($i = 1, 2$)

$$\chi_{i,\mathrm{L,T}}(\omega) = \mathrm{Im}\left\{\int\left(\frac{\mathrm{d}\mathbf{k}}{2\pi}\right)^3 C_i(\mathbf{k})\chi_{\mathrm{L,T}}(\mathbf{k},\omega)\right\} \quad (8)$$

where α is a proportionality constant which involves the incident intensity, divided by the fourth power of the wavelength of the scattered light [18]. This leads to a depolarization ratio of the form

$$\rho(\omega) = \frac{I_{\mathrm{VH}}(\omega)}{I_{\mathrm{VV}}(\omega)} = \left[\frac{4}{3} + 15\frac{\chi_{1,\mathrm{L}}(\omega)}{\chi_{2,\mathrm{L}}(\omega) + \frac{3}{2}\chi_{2,\mathrm{T}}(\omega)}\right]^{-1}. \quad (9)$$

We assume that the Pockels correlation functions are of Gaussian form (equation (2)) and introduce correlation lengths ξ_i and prefactors f_i ($i = 1, 2$) as $C_i(k) = f_i\tilde{C}_G(k)$.

Equations (4) and (5) form a set of self-consistent equations, which have to be solved numerically for the complex, frequency-dependent self-energy $\Sigma(\omega)$, using a suitable iteration procedure (usually 5–10 iterations are sufficient). For mathematical reasons a small positive imaginary part must be added to the frequency. The input into these equations are the unrenormalized sound velocities $v_{i,0}$, the Debye wavenumber k_{D}, the 'disorder parameter' γ (which must be smaller than its critical value γ_{c}) and the correlation length ξ_G of the fluctuations of the shear modulus. The direct numerical evaluation of the integrals (4) and (8) is numerically awkward, because of the singular denominator. Instead one has to use an integration-by-parts procedure, which is described in the appendix.

The dimensionless quantity $\tilde{\Sigma}(\omega) \equiv \Sigma(\omega)/v_{\mathrm{T},0}$ can be shown [14] to only depend on the dimensionless parameters

$v_{L,0}/v_{T,0}, \gamma$ and ξk_D. Furthermore for $\xi k_D \gg 1$ the function $\tilde{\Sigma}(\tilde{\omega})$ with the scaled frequency $\tilde{\omega} \equiv \omega/\xi/v_{T,0}$ becomes a universal function independent on ξk_D. This scaling property of the self-energy, which is proportional to the sound attenuation coefficient divided by the frequency [13], has been verified in a computer simulation [14].

Once the self-energy function $\Sigma(\omega)$ has been obtained it can be inserted into expression (6) for the DOS and into (7)–(9) for the Raman intensities and the depolarization ratio[6]. Here three additional model parameters enter: f_2/f_1, the ratio of the transverse and longitudinal Pockels constant fluctuations, and the two correlation lengths ξ_1 and ξ_2. As discussed below, the Pockels ratio can be fixed, because the average value of the depolarization ratio is a monotonic function of this ratio. The correlation lengths are set equal to that of the elastic constant fluctuations within the present analysis (although in principle they may take a different value).

The main prediction of the present theory for the dynamic susceptibility and the DOS is a cross-over of the self-energy function from a low-frequency regime, where it is essentially constant with a small imaginary part, to a high-frequency regime, where this function is strongly frequency-dependent. The low-frequency regime corresponds to a regime of Debye-like wave propagation. In this regime the imaginary part of the self-energy has a frequency dependence according to $\Sigma''(\omega) \propto \omega^3$, which leads to an ω^4 law for the sound attenuation (Rayleigh scattering). It has been proved recently that this is a generic feature for quenched–disordered harmonic systems [22].

In the high-frequency regime the DOS deviates from the Debye ω^2 law, which leads to the boson peak in the reduced DOS. The boson peak just marks the cross-over from the wave-like regime to the anomalous regime. This regime can be called 'random-matrix regime', because the eigenvalues of the dynamical matrix obey random-matrix statistics in this regime [9]. The energy currents do not propagate in a wave-like fashion but diffusively in this regime [23].

It has been shown in the literature [12–14] that the model of fluctuating elastic constants, which implies all these features, compares well with the experimental data. In particular it has been demonstrated that with increasing disorder γ and/or increasing correlation length ξ_G the boson peak shifts downwards with frequency and increases in intensity.

Concerning Raman scattering the present theory accounts for the different position and shape of the anomalous peaks in the Raman and in the neutron intensity [18]. This will be discussed in detail in the next section.

3. Experimental results

The $20Nb_2O_5$–$80NaPO_3$ and $40Nb_2O_5$–$60NaPO_3$ glasses were elaborated from $NaPO_3$ and Nb_2O_5 raw material using standard melting methods at 1100 °C in a platinum crucible, as previously described [24]. Inelastic neutron scattering spectra of the niobium-phosphate glass samples were measured at room temperature (295 K) with the time-of-flight spectrometer (TOFTOF) of the FRM II in Munich. The incident wavelength was 4.7 Å at an energy resolution of 0.1 meV. The niobium-phosphate glasses in powder form were filled in Nb double cylinders with 0.1 mm wall thickness. A vanadium standard in the same geometry was used to correct for detector efficiencies. The constituents of our material are all coherent scatterers of similar cross section. By averaging over the full accessible scattering angle (wavevector) range we obtain a $g(\nu)$ which gives an approximate spectral distribution of the vibrational modes [25] (effective DOS[7]). The time-of-flight data underwent the usual correction procedure, such as correction for the detector efficiencies, normalization to a vanadium scan, and subtraction of the empty cell contribution.

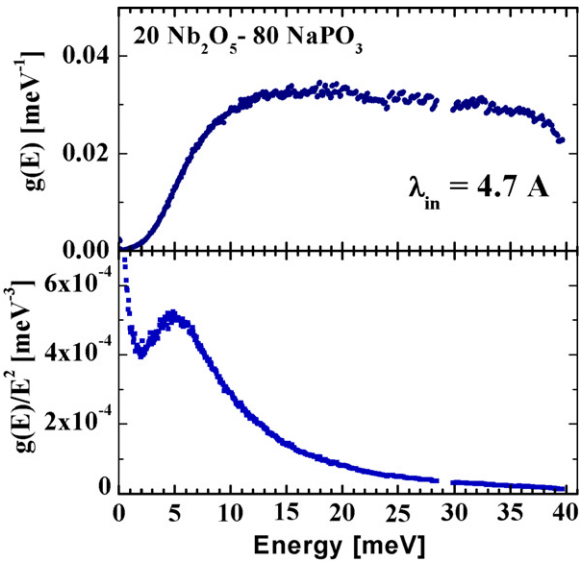

Figure 1. Low-frequency vibrational density of states of $20Nb_2O_5$–$80NaPO_3$ glass determined from thermal neutron scattering (top panel). The bottom panel shows the reduced density of states $g(E)/E^2$.

The DOS was obtained by an iterative procedure after correcting for the Debye–Waller factor and multiphonon contributions using the program IDA [26]. The resultant density of states curves $g(E)$ and $g(E)/E^2$ at 295 K are shown in figure 1. The Boson peak appears near 5 meV (40 cm^{-1}) as an enhancement of the reduced density of states over the Debye expectation.

For the spontaneous Raman measurements an Argon ion laser ($\lambda = 514.5$ nm) operating in single mode was employed as the excitation source. The Raman signal was collected in a backscattering geometry and spectrally analysed at a resolution of 1 cm^{-1} with a scanning double monochromator (U1000, JY Horiba), which was equipped with a photomultiplier detector and a single photon counting system. A linear polarizer

[6] Although the theoretical calculations for the DOS and the Raman intensities—as described in the text—are straightforward, they are too complicated to be implemented as 'push-button' least-mean-squares fit routines. Our model comparisons have been obtained by adjusting the parameters 'by hand'.

[7] In our theoretical analysis we took the effective DOS for the real one, although we are aware of possible deficiencies of the procedure used to extract the DOS from the coherent neutron data [27].

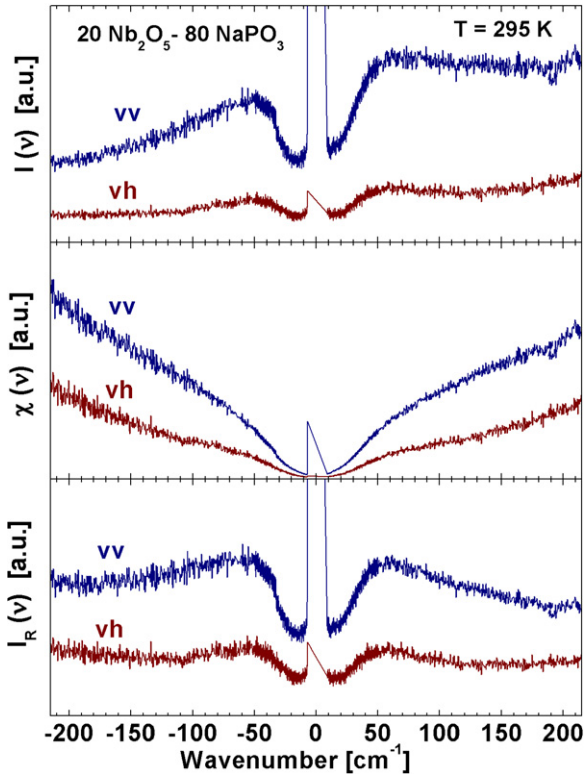

Figure 2. Intensity of Raman scattering (anti-Stokes and Stokes sides) in $20Nb_2O_5$–$80NaPO_3$ glass in three different representations: Raman intensity (top), Raman susceptibility (middle), and reduced Raman intensity (bottom).

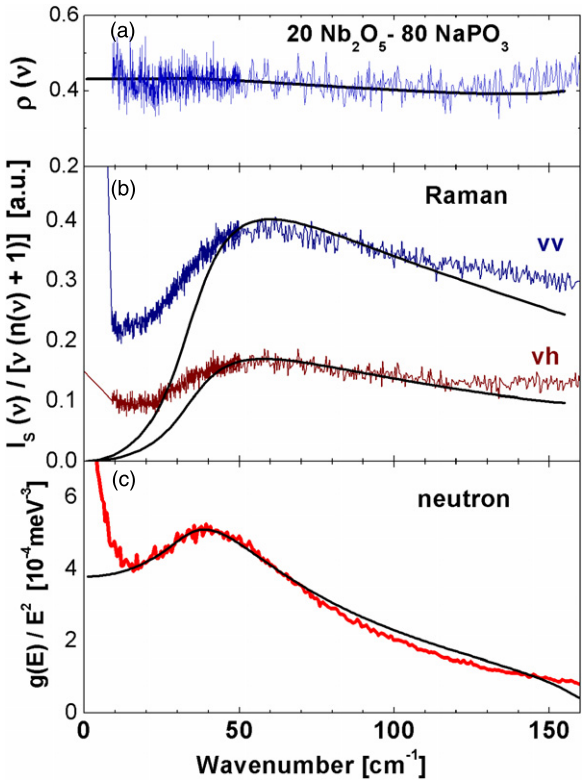

Figure 3. (a) Depolarization ratio $I_{VH}(\nu)/I_{VV}(\nu)$. (b) Reduced Raman intensities (upper: VV, lower: VH), compared with theory. (c) Reduced DOS $g(E)/E^2$, compared with theory, using the same parameters for the elastic model. These parameters are given in table 1.

Table 1. Model parameters.

Parameter	$20Nb_2O_5$–$80NaPO_3$	$40Nb_2O_5$–$60NaPO_3$
$k_D v_{T,0}/2\pi c$ (cm^{-1})	141	200
γ	$0.7\gamma_c$	$0.8\gamma_c$
$\xi_G = \xi_1 = \xi_2$	$1/(1.2k_D)$	$1/(4k_D)$
v_L/v_T	1.8	1.8
f_1/f_2	0.8	1.4

was mounted in front of the entrance slit of the spectrometer and kept in a fixed position for transmission of vertically polarized light. A polarizer and half-wave plate combination on the excitation side was used to select the polarization direction (vertical, V, or horizontal, H) of the incident light. The laser power was measured at the sample position for each polarization direction, and the acquired spectra were normalized to equal excitation intensity. Typical powers were 80 mW. As the data were recorded within 250 cm^{-1} of the laser light line (corresponding to 7 nm at 520 nm) no correction for grating efficiency and detector sensitivity was performed.

In figure 2 we show the Raman spectra on the Stokes and anti-Stokes side for VH as well as for VV scattering geometries. The middle and the bottom panels show the spectra, divided by the Bose factor and, to obtain the 'reduced intensity', further divided by the frequency ν. The Raman susceptibilities, presented in the middle panel, correspond to the predicted Raman gain [4]. The slight asymmetry at higher frequencies between Stokes and anti-Stokes sides of the susceptibility and reduced intensity curves may be attributed to a small wavelength dependence of the spectrometer/detector. Nevertheless, for the depolarization ratio this dependence cancels (see figures 3 and 4). In a similar way we obtained VV and VH spectra for a material of the composition $40Nb_2O_5$–$60NaPO_3$.

4. Model calculations and discussion

In figure 3 the Raman data for $20Nb_2O_5$–$80NaPO_3$ are compared with the reduced DOS $g(\omega)/\omega^2$. It is clearly seen, that the latter quantity has a maximum near 40 cm^{-1}, whereas the maximum of the Raman data occurs near 55 cm^{-1}. Results of theoretical calculations according to equations (2)–(9) are represented by the full lines. To provide a stringent test for the theory it is essential to have light-scattering data for VH as well as for VV geometries. We estimated the ratio of the (renormalized) sound velocities to be $v_L/v_T \sim 1.8$. This corresponds to an unrenormalized ratio of $v_{L,0}/v_{T,0} = 1.7$, which leads to a critical disorder parameter $\gamma_c = 0.198 v_{T,0}^4$. (The absolute velocity scale does not enter.) The other fit parameters are displayed in table 1. The values of the correlation length used in the theoretical calculations are given in terms of the Debye cutoff k_D. If one uses the formula units of the material as a coarse-graining unit for the Debye model, k_D^{-1} should be a fraction of a nanometre. The absolute value of the correlation length cannot be obtained by the fitting

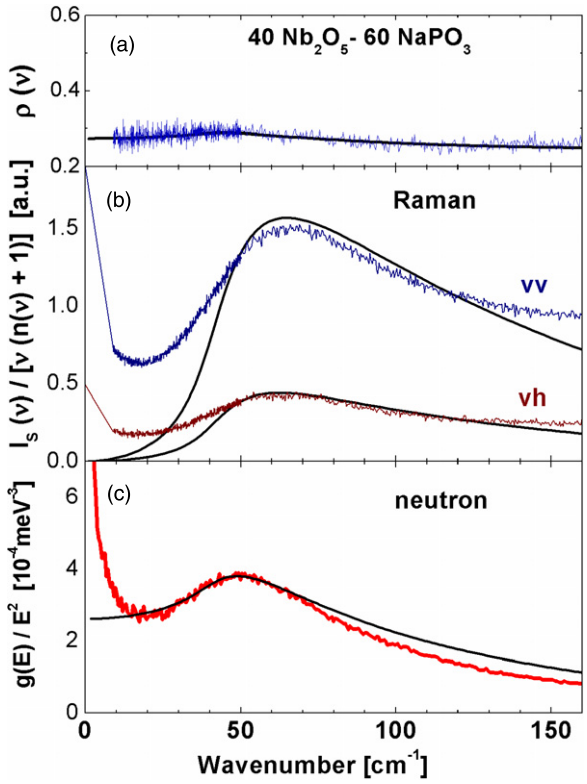

Figure 4. (a) Depolarization ratio $I_{VH}(\nu)/I_{VV}(\nu)$. (b) Reduced Raman intensities (upper: VV, lower: VH), compared with theory. (c) Reduced DOS $g(E)/E^2$, compared with theory, using the same parameters for the elastic model. These parameters are given in table 1.

procedure. The strength of our model is in relating the neutron and Raman spectrum and obtaining relative changes of the model parameters, if sample parameters are changed.

It is remarkable that the theory reproduces not only the absolute value, but also the spectral shape of the depolarization ratio $\rho(\nu)$. The depolarization ratio varies between 0.44 and 0.39 over the frequency range from 10 to 150 cm^{-1}. As the value of $\langle\rho\rangle$ is controlled by the ratio of the mean-square Pockels constant fluctuations $\langle\Delta a_1^2\rangle/\langle\Delta a_2^2\rangle$, which turned out to be ∼0.8, we conclude that the 'longitudinal' fluctuations Δa_1 are slightly weaker than the 'transverse' fluctuations Δa_2 in the niobium-phosphate glass. This reflects the structural and geometrical characteristics of the scatterers. Different values for $\langle\rho\rangle$ are expected for glasses with different local structure, which is consistent with observed values from 0.25 up to the possible maximum value of 0.75 in a range of materials [17].

In figure 4 the Raman data for $40Nb_2O_5$–$60NaPO_3$ are compared with the reduced DOS $g(E)/E^2$. Again the theory is in good agreement with the Raman spectrum for both polarizations and the neutron data. The parameter γ is fixed by the density of states from neutron scattering, and the Raman data provide a value for the fluctuations in the elasto-optical constants (table 1). Compared to the 20% data (figure 3) the boson peak occurs at higher frequencies (maxima at 49 cm^{-1} in the reduced density of states and 60 cm^{-1} in the Raman spectra). This corresponds to a smaller γ parameter and a smaller correlation length (see table 1). With the increase in Nb concentration the depolarization ratio is slightly lower, indicating a more pronounced contribution of the longitudinal Pockels constant fluctuation. Structurally, in the niobium-phosphate glasses progressive introduction of Nb_2O_5 may lead to the formation of corner-shared NbO_6 octahedra chains and a 2d phospho-niobate network [28]. This in turn would decrease the correlation length in the fluctuations of the elasto-optical constants for the same Debye wavenumber k_D.

We note that in contrast to the present theory the previous theoretical scheme utilized by the Raman community to discuss the low-frequency Raman enhancement, namely the 'corrected Shuker–Gammon formula' [15], did not permit one to obtain microscopic information about the vibrational and elasto-optic properties of the materials. Neither did it make any statement about the depolarization ratio. Within the theoretical framework used here one can unambiguously determine the ratio of the mean-square Pockels constant fluctuations from the depolarization ratio. This is also the case in the theory of Martin and Brenig [21] for the Raman spectrum of a Debye solid with spatially fluctuating Pockels constants. However, to also be in agreement with the density of states from inelastic neutron scattering and the frequency dependence of the depolarization ratio, a unified framework that takes into account the vibrational excitations of a disordered (non-Debye) solid is necessary. In the theory of reference [12], employed here, this is achieved by including spatial fluctuations of the elastic constants.

Finally, we would like to comment on the 'offset' of the Raman data in comparison with the theoretical model below the low-frequency wing of the boson peak. Our theory shares the feature of the theory of Martin and Brenig [21] that the intensity vanishes with $\nu \to 0$ as $I(\nu) \propto \nu^2$. In many experiments, instead, a constant offset in the intensity is observed, which is roughly proportional to the temperature. This contribution can be attributed to the presence of anharmonicity in the vibrational dynamics. A recent theoretical work on the vibrational spectrum of disordered solids that includes anharmonic effects [29] predicts a sound attenuation constant which is proportional to the squared frequency and the temperature. If this contribution is added to the self-energy in the theory of Raman scattering we obtain a low-frequency enhancement of the intensity, which is constant and proportional to temperature. The influence of anharmonic interactions provides an avenue for further research.

5. Conclusion

We have shown that the measured inelastic neutron and low-frequency Raman spectra of niobium-phosphate glasses can be quantitatively described by a unified model that includes spatial fluctuations in both the elastic constants of the disordered medium and the elasto-optical (Pockels) constants. The value of the depolarization ratio for Raman scattering is determined by the mean-square Pockels constant fluctuations, while its frequency dependence is modulated by the vibrational disorder of the elastic medium.

Acknowledgments

We thank T Cardinal for help with the sample preparation. This work was supported in part by NSF grant DMR-0421253 and by the Neutronenquelle 'Heinz Maier-Leibnitz' (FRM II) through the allocation of beam time. AS and WS are grateful for travel support through the BaCaTec program.

Appendix

We want to calculate the reciprocal space integral occurring in equations (4) and (8):

$$\chi(z) = \frac{1}{(2\pi)^3}\int_{|\mathbf{k}|<k_\mathrm{D}} \mathrm{d}^3\mathbf{k}\,\tilde{C}(k)\frac{k^2}{-z^2+k^2[v^2-\Sigma(z)]} \tag{10}$$

with $z = \omega + \mathrm{i}\epsilon$, and one has to insert the appropriate quantities $v \equiv v_{\mathrm{L,T},0}$ and $\Sigma \equiv \Sigma_{\mathrm{L,T}}$, respectively. Defining $A_\xi = \frac{1}{(2\pi)^3}\int_{|\mathbf{k}|<k_\mathrm{D}} \mathrm{d}^3\mathbf{k}\,\mathrm{e}^{-k^2\xi^2}$, we have $\tilde{C}(k) = \frac{1}{A_\xi}\mathrm{e}^{-k^2\xi^2}$, and equation (10) becomes

$$\chi(z) = \frac{1}{2\pi^2 A_\xi[v^2-\Sigma(z)]}\int_0^{k_\mathrm{D}} \mathrm{d}k\,\frac{\mathrm{e}^{-k^2\xi^2}k^4}{-\underbrace{\frac{z^2}{v^2-\Sigma(z)}}_{s^2}+k^2}$$

$$= \frac{1}{2\pi^2[v^2-\Sigma(z)]}\left[\tilde{C}(k_\mathrm{D})\,k_\mathrm{D}^3\,\varphi(s/k_\mathrm{D}) + 2\xi^2\int_0^{k_\mathrm{D}} \mathrm{d}\tilde{k}\,\tilde{C}(\tilde{k})\,\tilde{k}^4\,\varphi(s/\tilde{k})\right] \tag{11}$$

where the second line follows from an integration by parts. The auxiliary function $\varphi(u)$ is given by

$$\varphi(u) = \int_0^1 \mathrm{d}\kappa\,\frac{\kappa^4}{\kappa^2-u^2} = \left[\frac{1}{3}+u^2\left(1+\frac{u}{2}[\ln(1-u)-\ln(-1-u)]\right)\right]. \tag{12}$$

The branch cut of the complex logarithm has to be taken along the negative real axis. As this function is not singular, the numerical integral on the right-hand side of equation (11) can be readily performed.

References

[1] Jäckle J 1981 *Amorphous Solids: Low-Temperature Properties* ed W A Phillips (Heidelberg: Springer) p 135
[2] Petry W and Wuttke J 1995 *Transp. Theory Stat. Phys.* **24** 1075
[3] Carabatos-Nedelec C 2001 Raman scattering of glass *Handbook of Raman Spectroscopy* ed I R Lewis and H G M Edwards (New York: Dekker) p 423
[4] Stegeman R, Jankovic L, Kim H, Rivero C, Stegeman G, Richardson K, Delfyett P, Guo Y, Schulte A and Cardinal T 2003 *Opt. Lett.* **28** 1126
[5] Binder K and Kob W 2005 *Glassy Materials and Disordered Solids* (Singapore: World Scientific)
[6] Horbach J *et al* 2001 *Eur. Phys. J.* B **19** 531
[7] Nakayama T 2002 *Rep. Prog. Phys.* **65** 1195
[8] Gurevich V L *et al* 2003 *Phys. Rev.* B **67** 094203
[9] Schirmacher W, Diezemann G and Ganter C 1998 *Phys. Rev. Lett.* **81** 136
[10] Taraskin S N, Loh Y H, Natarajan G and Elliott S R 2001 *Phys. Rev. Lett.* **86** 1255
[11] Lubchenko V and Wolynes P 2003 *Proc. Natl. Acad. Sci. USA* **100** 1515
[12] Schirmacher W 2006 *Europhys. Lett.* **73** 892
[13] Schirmacher W, Ruocco G and Scopigno T 2007 *Phys. Rev. Lett.* **98** 025501
[14] Schirmacher W, Schmid B, Tomaras C, Viliani G, Baldi G, Ruocco G and Scopigno T 2008 *Phys. Status Solidi* c **5** 862
[15] Shuker R and Gammon R 1970 *Phys. Rev. Lett.* **25** 222
[16] Lannin J S 1977 *Phys. Rev.* B **15** 3863
Duval E *et al* 1990 *J. Phys.: Condens. Matter* **2** 10227
Benassi P *et al* 1991 *Phys. Rev.* B **44** 11734
Zemlyanov M G *et al* 1991 *Sov. Phys.—JETP* **74** 151
Archibat T *et al* 1993 *J. Chem. Phys.* **99** 2046
Sokolov A P *et al* 1993 *Phys. Rev.* B **48** 7692
Duval E *et al* 1993 *Phys. Rev.* **48** 16785
Ohsaka T *et al* 1994 *Phys. Rev.* **50** 9569
Surovtsev N V *et al* 1999 *Phys. Rev. Lett.* **82** 4476
Novikov V N and Surovtsev N V 1999 *Phys. Rev.* B **59** 38
Saviot L *et al* 1999 *Phys. Rev.* B **60** 18
Duval E *et al* 1999 *Phil. Mag.* B **79** 2051
Hehlen B *et al* 2000 *Phys. Rev. Lett.* **84** 5355
Surovtsev N V 2001 *Phys. Rev.* B **64** 061102
Ivanda M *et al* 2001 *Solid State Commun.* **117** 423
Surovtsev N V and Sokolov A P 2002 *Phys. Rev.* B **66** 054205
Surovtsev N V *et al* 2003 *Phys. Rev.* B **67** 024203
Surovtsev N V *et al* 2004 *J. Phys.: Condens. Matter* **16** 223
Fontana *et al* 2007 *J. Phys.: Condens. Matter* **19** 205145
Surovtsev N V 2004 *Phys. Status Solidi* c **1** 2867
Courtens E *et al* 2003 *J. Phys.: Condens. Matter* **15** S1279
Yannopoulos S N and Andrikopoulos K S 2004 *J. Chem. Phys.* **121** 4747
Malinovsky V K *et al* 1990 *Europhys. Lett.* **11** 43
Tao N J, Li G, Chen X, Du W M and Cummins H Z 1991 *Phys. Rev.* A **44** 6665
[17] Yannopoulos S N and Papatheodorou G N 2000 *Phys. Rev.* B **62** 3728
[18] Schmid B and Schirmacher W 2008 *Phys. Rev. Lett.* **100** 137402
[19] Guo Y, Nonnenmann S, Schulte A, Rivero C, Richardson K, Stegeman R, Stegeman G and Cardinal T 2004 *Conf. on Lasers and Electro-Optics Technical Digest (OSA)* CThP2
[20] Landau L D and Lifshitz E M 1960 *Electrodynamics of Continuous Media* (New York: Pergamon) p 391
[21] Martin A J and Brenig W 1974 *Phys. Status Solidi* b **64** 163
[22] Ganter C and Schirmacher W 2010 *Phys. Rev.* B **82** 094205
[23] Allen P B and Feldman J L 1993 *Phys. Rev.* B **48** 12581
Feldman J L, Kluge M D, Allen P B and Wooten F 1993 *Phys. Rev.* B **48** 189
[24] Schulte A, Guo Y, Schirmacher W, Unruh T and Cardinal T 2008 *Vib. Spectrsoc.* **48** 12
[25] Buchenau U 1985 *Z. Phys.* B **58** 181
[26] Wuttke J http://sourceforge.net/projects/frida/
[27] Taraskin S N and Elliott S R 1997 *Phys. Rev.* B **55** 117
[28] Cardinal T, Fargin E, Le Flem G and Leboiteux S 1997 *J. Non-Cryst. Solids* **222** 228
[29] Tomaras C, Schmid B and Schirmacher W 2010 *Phys. Rev.* B **81** 104206